Research Article

Rapid Communications in Mass Spectrometry

Received: 30 January 2013 Revised: 16 April 2013 Accepted: 24 April 2013 Published online in Wiley Online Library

Rapid Commun. Mass Spectrom. **2013**, 27, 1619–1630
(wileyonlinelibrary.com) DOI: 10.1002/rcm.6611

Selective collision-induced fragmentation of *ortho*-hydroxybenzyl-aminated lysyl-containing tryptic peptides

E. S. Simon*, P. G. Papoulias and P. C. Andrews

Departments of Biological Chemistry, Bioinformatics, and Chemistry, University of Michigan, Ann Arbor, 48103

RATIONALE: In protein studies that employ tandem mass spectrometry the manipulation of protonated peptide fragmentation through exclusive dissociation pathways may be preferred in some applications over the comprehensive amide backbone fragmentation that is typically observed. In this study, we characterized the selective cleavage of the side-chain C_ζ–N_ε bond of peptides with *ortho*-hydroxybenzyl-aminated lysine residues.
METHODS: Internal lysyl residues of representative peptides were derivatized via reductive amination with *ortho*-hydroxybenzaldehyde. The modified peptides were analyzed using collision-induced dissociation (CID) on an Orbitrap tandem mass spectrometer. Theoretical calculations using computational methods (density functional theory) were performed to investigate the potential dissociation mechanisms for the C_ζ–N_ε bond of the derivatized lysyl residue resulting in the formation of the observed product ions.
RESULTS: Tandem mass spectra of the derivatized peptide ions exhibit product peaks corresponding to selective cleavage of the side-chain C_ζ–N_ε bond that links the derivative to lysine. The *ortho*-hydroxybenzyl derivative is released either as a neutral moiety [$C_7H_6O_1$] or as a carbocation $[C_7H_7O_1]^+$ through competing pathways (retro-*Michael* versus Carbocation Elimination (CCE), respectively). The calculated transition state activation barriers indicate that the retro-*Michael* pathway is kinetically favored over CCE and both are favored over amide cleavage.
CONCLUSIONS: The application of *ortho*-hydroxybenzyl amination is a promising peptide derivatization scheme for promoting selective dissociation pathways in the tandem mass spectrometry of protonated peptides. This can be implemented in the rational development of peptide reactive reagents for applications that may benefit from selective fragmentation paths (including crosslinking or MRM reagents). Copyright © 2013 John Wiley & Sons, Ltd.

When analyzed using low-energy collision-induced dissociation (CID) tandem mass spectrometry (MS/MS) protonated peptides typically fragment along the amide backbone, producing spectra containing a series of peaks whose *m/z* differentials correspond to differences in amino acid residues within the peptide.[1] Interpretation of the data can be used to extract amino acid sequence information and/or post-translational modifications. Proteomics takes advantage of the partially predictable nature of CID-based peptide fragmentation on a large scale by comparing thousands of MS/MS spectra against thousands of *in silico* peptide sequences generated from proteome databases.[2–4] This technique relies upon the presence of comprehensive series of sequence ion peaks from MS/MS spectra to ensure confident peptide assignments. However, there are a number of other applications of CID to peptide analysis where comprehensive amide backbone cleavage is not necessarily desirable. Two notable examples are the application of CID to cross-linked peptides and multiple reaction monitoring (MRM). Cross-linking of proteins is typically applied to elucidate protein complex structures/arrangements and interactions.[5] However, MS/MS spectra of cross-linked peptides exhibit complex, overlapping series of sequence ion peaks which are difficult to interpret.[6] MRM is currently used in proteomics as a targeted approach to increase sensitivity and reduce analysis time.[7] The sensitivity of the MRM technique relies on the signal intensity of one or multiple selected product ions generated from CID of a targeted precursor peptide ion (referred to as MRM transitions). However, the selected product ion(s) contain only a small fraction of the total product ion current as the rest is diluted throughout a much larger population of amide cleavage product ions.

Recently, solutions to these limitations have been presented which rely upon chemical modifications that induce selective and predictable cleavage events upon activation of the derivatized peptide ion. Reid and coworkers have characterized the fragmentation of methionyl side-chain sulfonium-ion-derivatized peptides which exhibit a characteristic exclusive cleavage event that eliminates the derivative moiety.[8] The authors applied knowledge of this distinctive fragmentation behavior to the development of a sulfonium-ion-containing cross-linking reagent.[9] The cross-linked peptides fragment strictly at bonds adjacent to the sulfonium component of the cross-linker allowing the two peptides to dissociate as intact peptide ions which can be subsequently interrogated independently via multi-stage tandem mass spectrometry. A conceptually similar cross-linker that promotes selective fragmentation has also been described recently that is based on chemistry used in Edman degradation.[10]

* *Correspondence to:* Correspondence to: E. S. Simon, 3561 Lexington Circle, Dexter, MI 48130, USA.
E-mail: ess2011.simon@gmail.com

Similarly, the MRM technique could benefit from limiting the number of active fragmentation channels to a minimal number that represent the majority of the product ion current. It was demonstrated recently that chemical derivatization of peptides which induce selective, site-specific cleavage reactions of protonated peptides can improve the sensitivity of MRM assays considerably.[11] In that study, N-terminal phenylthiocarbamoylation of peptides was shown to produce predominantly the b_1 and corresponding y_{n-1} ion.[11] This essentially concentrates the product ion current to those two associated product ions and it was demonstrated that selecting the $[MH_n]^{n+} \rightarrow b_1$ and/or $[MH_n]^{n+} \rightarrow y_{n-1}$ transitions for the modified peptides increased the MRM signal two orders of magnitude over transitions selected for the corresponding unmodified peptide. In another study, N-terminal sulfonation of protonated peptides was employed to restrict product ion formation to the y-ion type.[12] By manipulating fragmentation to exclude the formation of other product ion types, a greater flux of ion current can be channeled through the pathways that yield y-ion type product ions; thus increasing their signal intensities and the sensitivity of the MRM technique.

The benefits to restricting peptide fragmentation to predictable pathways are evident for applications like cross-linking reagents and MRM assays and suggest that the need for developing other chemical approaches that manipulate the formation and relative abundance of product ions as well as providing additional properties is warranted. Our group recently described the CID fragmentation characteristics of benzyl-aminated lysyl-containing peptides.[13] Evidence for two main charge-dependent fragmentation pathways was observed. One pathway resulted in the formation of sequence ions originating from amide backbone cleavage ($b_n - y_m$ pathway). The second pathway led to the formation of an intact, unmodified peptide product ion, $[(MH_2)^{2+} - (C_7H_7)^+]^+$, originating from the lysyl side-chain elimination of the benzyl moiety as a benzylic carbocation, $[C_7H_7]^+$, through a mechanism we described as the carbocation elimination pathway (CCE). For triply charged precursor ions, products originating from the CCE pathway ($[(MH_3)^{3+} - (C_7H_7)^+]^{2+}$ and $[C_7H_7]^+$) were observed exclusively. We presented evidence that the CCE pathway was contingent upon protonation of the side-chain secondary ε-amino group of the benzyl-aminated lysyl residue which led to heterolytic cleavage of the C_ζ–N_ε bond releasing the benzylic carbocation. In a follow-up study, we investigated the effect of various chemical substituents on the benzyl ring on the proportion of CCE versus $b_n - y_m$ products observed.[14] The relative extent of the CCE pathway was determined by the ability of the substituent to stabilize the positive charge on the incipient carbocation. Thus, electron-donating substituents promoted increased dissociation via the CCE pathway. This was exhibited through a strong correlation between the intensity ratios of CCE versus $b_n - y_m$ products formed and the Hammett substituent constant of the substituent on the benzyl ring. Therefore, Hammett methodology can be applied to insert substituents with specific electronic properties to predictably manipulate the relative formation of CCE versus $b_n - y_m$ products. Such versatility could allow for designing new cross-linking or quantification tagging reagents with desirable and predictable fragmentation tendencies.

For benzyl-aminated peptides, doubly protonated peptides do not exhibit selective cleavage of the C_ζ–N_ε bond of the derivatized lysyl residue like that which is observed for triply protonated peptides. Manipulating fragmentation to promote selective cleavage of the C_ζ–N_ε bond regardless of charge state was one of our goals in assessing substituent effects on the benzyl ring. Toward that goal, this study describes our investigation of the fragmentation of the *ortho*-hydroxybenzyl analogs. *ortho*-Hydroxybenzyl derivatization was considered due to the known preferential cleavage of 2-hydroxybenzyl-*N*-pyrimidinylamine derivatives at the analogous C–N bond via a retro-*Michael*-type mechanism.[15] For the *ortho*-hydroxybenzyl-aminated peptides analyzed in this study, cleavage of the C_ζ–N_ε bond was observed almost exclusively for doubly and triply protonated precursors. The retro-*Michael*-type dissociation channel (involving intramolecular substitution by a proton originating from the *ortho*-hydroxyl group of the benzyl ring) eliminates the hydroxybenzyl moiety as a neutral species, $[C_7H_6O_1]$. Additionally, the CCE pathway is also observed complimenting the retro-*Michael* reaction by cleaving the C_ζ–N_ε bond and eliminating the moiety as a carbocation $[C_7H_7O_1]^+$. Products from the CCE pathway are observed primarily from triply protonated precursors while products from the retro-*Michael* pathway are observed from both doubly and triply protonated precursors. This derivatization scheme could be further developed to suit applications that may benefit from selective fragmentation characteristics.

EXPERIMENTAL

Materials

Unless otherwise stated, all reagents were purchased from Sigma-Aldrich (St. Louis, MO, USA). The N-terminally acetylated peptides used in this study were synthesized by the Protein Structure Facility, part of the Biomedical Research Core Facilities, at the University of Michigan Medical School (Ann Arbor, MI, USA).

Preparation of tryptic peptides containing hydroxybenzyl-derivatized lysyl residues

Peptides (5 μg) were dissolved in 250 μL of 200 mM sodium acetate (pH ~5.7) with 20% methanol. Approximately 50 mmol of either *ortho*- or *meta*-hydroxybenzaldehyde was then added. The resulting Schiff bases were reduced to secondary amines by adding 5 μL of 1 M sodium borohydride. The reduction reaction was allowed to proceed undisturbed at room temperature for 45 min in a fume hood in the dark. The reaction was quenched by adding 1 mL of 0.1% trifluoroacetic acid. The reacted peptides were desalted using a Strata-X reversed-phase C18 cartridge obtained from Phenomenex (Torrance, CA, USA) according to the manufacturer's instructions. The desalted peptides were dried and redissolved in 200 μL of 100 mM triethylammonium bicarbonate (pH ~8.5). Then 1 μg of L-(tosylamido-2-phenyl)ethyl chloromethyl ketone treated trypsin, obtained from Worthington Biochemical Corp. (Lakewood, NJ, USA), was added to the peptide solution and incubated at 37 °C overnight. The digested peptides

Rapid Communications in Mass Spectrometry

were desalted as described above, dried to completion, and redissolved in 50 μL of 25% acetonitrile/0.1% formic acid (v/v) for analysis with nanospray mass spectrometry.

Mass spectrometry

Peptides were analyzed with a hybrid linear quadrupole ion trap–orbitrap mass spectrometer (LTQ-Orbitrap XL; ThermoFisher Scientific, Inc., San Jose, CA, USA). They were introduced by infusion using a TriVersa Nanomate nanospray ionization source from Advion BioSciences (Ithaca, NY, USA). Peptides were delivered with a pneumatic displacement pressure of 0.45 psi and an applied spray voltage of 1.63 kV. The heated capillary temperature was set at 200 °C. Monoisotopic precursor ions were selected for multi-stage tandem mass spectrometric acquisition using an isolation window of 3.0 (*m/z* units) and excitation energy settings of 35 for both MS^2 and MS^3 spectra. All CID product ion spectra were collected in FT (Orbitrap) mode for high mass accuracy (<10 ppm) and peak resolution (30000 at *m/z* 400).

Computational methods

Total energy calculations were performed using density functional theory (DFT) with electron correlations treated with the B3LYP hybrid functional. Atomic orbitals were described using the split-valence double-zeta functions with d and p polarization functions added to both heavier and lighter atoms and diffuse functions added for the heavier atoms (i.e. 6-31 + G(d,p)). The model peptide 2-[(aminoacetyl) amino]-6-(2-hydroxybenzyl)amino]hexanoic acid was used for theoretical calculations. Transition state barriers were determined by scanning the potential energy surface at the B3LYP level of theory using the 6-31G + (d,p) basis set . The retro-*Michael* pathway for the case of protonation of the secondary amine was examined by exploring the potential energy surface by first dragging the precursors to an intermediate configuration by increasing the length of the C_ζ–N_ε bond (the bond that is cleaved during the reaction) incrementally while allowing all other degrees of freedom to relax. With the C_ζ–N_ε bond stretched by 0.9 Å above its equilibrium length, the relative configuration of the two fragments was adjusted through a rotation which brought the *ortho*-hydroxyl group of the hydroxybenzyl ring closer to the N_ε atom of the secondary amine. The potential energy surface was subsequently scanned by increasing the O–H distance until the H atom relaxed to an equilibrium bond length with the N_ε atom of the secondary ε-amino group. The exploration of the potential energy surface for the retro-*Michael*-type pathway (for the case that the secondary ε-amino group was neutral) proceeded in two steps. First, a scan of the potential energy surface was perfomed by incrementing the distance of the O–H bond. Once the H atom was within 0.1 Å of its equilibrium bond length to the N_ε atom of the secondary amine, the scan of the potential energy surface proceeded by increasing the length of the C_ζ–N_ε bond incrementally. The CCE pathway was investigated in a similar manner with a scan of the potential energy surface by increasing the length of the C_ζ–N_ε bond incrementally while allowing all other degrees of freedom to relax. Optimized structures were subjected to harmonic vibrational frequency analysis and visualized using the software package GaussView 3.0. All calculations were done using the Gaussian 2003 molecular modeling software package.[16]

RESULTS AND DISCUSSION

MS/MS of multiply charged peptides derivatized at lysyl residues via reductive amination with *ortho*-hydroxybenzaldehyde

As depicted in Fig. 1 for *o*-hydroxybenzaldehyde, peptides containing N-terminally acetylated arginine and a single, internal lysyl residue were derivatized via reductive amination with *o*-hydroxybenzaldehyde and then digested with trypsin. This approach allowed for the preparation of tryptic peptides with the modification exclusively on the ε-amino groups of internal lysyl residues while leaving the N-termini unmodified (Fig. 1, inset). The residue mass of the modified lysyl is 234.137 Da ($C_{13}H_{18}N_2O_2$).

In our previous work,[13] we showed that the MS/MS spectra of doubly charged, unsubstituted benzyl-aminated peptides exhibited peaks representing two dominant fragmentation pathways: (1) the $b_m - y_n$ pathway producing amide cleavage products and (2) the carbocation elimination (CCE) pathway which involves the direct heterolytic cleavage of the C_ζ–N_ε bond of the derivatized lysyl residue producing a benzylic carbocation, $[C_7H_7]^+$, and the remaining intact peptide product ion after dissociation of the carbocation, $[(MH_n)^{n+} - (C_7H_7)^+]^{(n-1)+}$ (Scheme 1). For triply charged benzyl-aminated peptides, product ion peaks from the CCE pathway were observed almost exclusively. It was determined that protonation of the secondary ε-amino group of the derivatized residue was required for the CCE pathway to become a viable fragmentation channel.

Figures 2(A) and 2(B) display tandem mass spectra of the doubly and triply charged precursor ions of the peptide $HAK_{o\text{-}OH}LGR$, respectively (where $K_{o\text{-}OH}$ represents an *o*-hydroxybenzyl-aminated lysyl residue). For the doubly charged precursor, a single peak representing a doubly charged product ion, $[(MH_2)^{2+} - (C_7H_6O_1)]^{2+}$, was observed exclusively at *m/z* 341.21 and corresponds to neutral loss of 106.04 Da. The *m/z* 341.21 ratio matches the theoretical *m/z* ratio of the unmodified peptide HAKLGR as a doubly

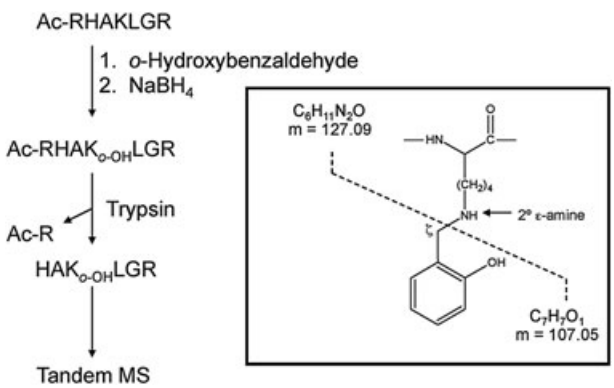

Figure 1. Workflow for the preparation of *ortho*-hydroxybenzyl-derivatized, tryptic peptides via reductive amination of lysyl residues (K^*) with *ortho*-hydroxybenzaldehyde. Inset: structure of *ortho*-hydroxybenzyl-aminated lysyl residue.

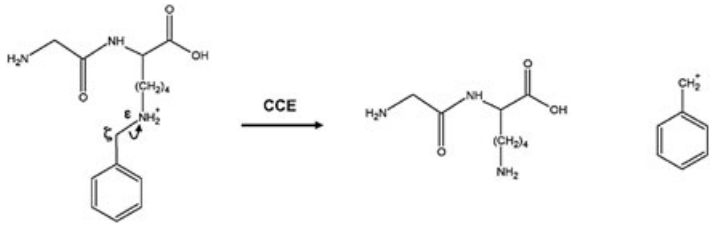

Scheme 1. The CCE pathway. A charge-directed elimination reaction contingent upon protonation of the secondary ε-amino group and proceeds via an unsymmetrical, heterolytic cleavage of the C_ζ-N_ε bond resulting in the dissociation of a benzylic carbocation.

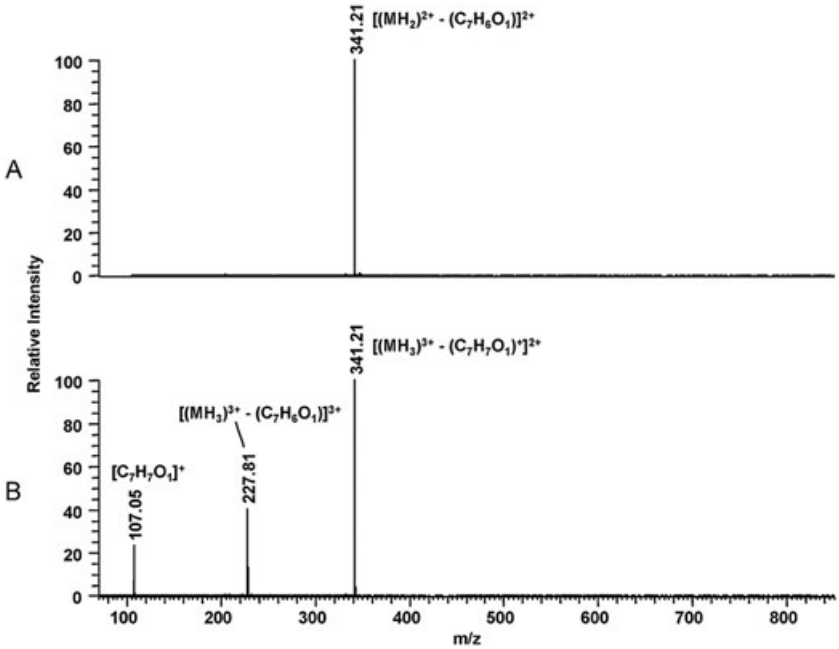

Figure 2. CID tandem mass spectra of the *ortho*-hydroxybenzyl-derivatized peptide $HAK_{o\text{-}OH}LGR$ (where $K_{o\text{-}OH}$ represents the *ortho*-hydroxybenzyl-aminated lysyl residue). (A) CID MS/MS product ion spectrum of the doubly charged $[MH_2]^{2+}$ precursor ion. (B) CID MS/MS product ion spectrum of the triply charged $[MH_3]^{3+}$ precursor ion.

protonated peptide ion. MS^3 spectra of the $[(MH_2)^{2+} - (C_7H_6O_1)]^{2+}$ product ion confirmed that the lysyl residue reclaimed its endogenous primary ε-amino structure after fragmentation (data not shown). Although it is fairly straightforward to interpret that the eliminated neutral species $[C_7H_6O_1]$ represents the hydroxybenzyl moiety after cleavage of the C_ζ–N_ε bond (refer to Fig. 1), it is apparent that the CCE pathway is not the active fragmentation channel producing the $[(MH_2)^{2+} - (C_7H_6O_1)]^{2+}$ product ion. Direct cleavage of the C_ζ–N_ε bond via the CCE pathway would produce a singly charged hydroxybenzyl carbocation $[C_7H_7O_1]^+$ (theoretical *m/z* 107.05) and a singly charged peptide product ion, $[(MH_2)^{2+} - (C_7H_7O_1)^+]^+$ (theoretical *m/z* 681.42).

Figure 2(B) displays the tandem mass spectrum of the triply charged peptide $HAK_{o\text{-}OH}LGR$. Like the spectrum shown in Fig. 2(A) for the doubly charged precursor ion, the triply charged precursor ion also produces a doubly charged product ion of *m/z* 341.21. However, in this case the loss of a charge unit concomitant with the loss of a mass of 107.05 Da ($[C_7H_7O_1]^+$) from the precursor suggests that the CCE pathway is the fragmentation channel producing the product ion $[(MH_3)^{3+} - (C_7H_7O_1)^+]^{2+}$ at *m/z* 341.21. The presence of the peak at *m/z* 107.05 representing the carbocation $[C_7H_7O_1]^+$ supports this assignment. The peak at *m/z* 227.81 represents a triply charged peptide product ion, $[(MH_3)^{3+} - (C_7H_6O_1)]^{3+}$, showing that the pathway leading to loss of $[C_7H_6O_1]$ (106.04 Da) is also an active fragmentation channel for triply charged precursors and competes with the CCE pathway. The *m/z* ratios 341.21 and 227.81 correspond to the calculated unmodified *m/z* ratios for the peptide HAKLGR as doubly and triply charged peptides, respectively. This suggests that the lysyl residue adopts its normal primary ε-amino structure after cleavage of the C_ζ–N_ε bond from both fragmentation mechanisms and this was confirmed via the acquisition

Rapid Communications in Mass Spectrometry

ofMS^3 spectra of the corresponding product ions (data not shown).

Figures 3(A) and 3(B) display tandem mass spectra for the doubly and triply charged precursor ions of the peptide $IGK_{o\text{-}OH}GVAR$, respectively. This peptide exhibits a very similar fragmentation pattern to $HAK_{o\text{-}OH}LGR$; however, one slight difference to emphasize is that there is evidence that the CCE pathway is an active fragmentation channel for the doubly charged precursor of $IGK_{o\text{-}OH}GVAR$ represented by the peak at *m/z* 700.45 in Fig. 3(A). This peak corresponds to a singly charged peptide product ion after elimination of a hydroxybenzyl carbocation, $[(MH_2)^{2+} - (C_7H_7O_1)^+]^+$, and also matches the calculated *m/z* ratio of the singly charged peptide IGKGVAR.

Proposed mechanisms of C_ζ–N_ε bond cleavage

Alkylammonium ions typically undergo unimolecular dissociation through loose ion-neutral complex intermediates.[17,18] *N*-Alkylpyridinium cations can fragment from such intermediates to form a pyridinium cation and an olefin[17] or, alternatively, a neutral pyridine and a carbocation.[18] For *N*-benzylpyridinium[19,20] and other benzylammonium ions,[21] the formation of pyridine (or the corresponding neutral amine) and a benzylic carbocation is observed. The latter reactions proceed through an almost indistinguishable transition state to form a loose ion-neutral complex intermediate before separation of the carbocation from the amine.[18,21] As shown in our previous study, when *N*-benzyl-*N*-alkylamines are incorporated into more complex ions, such as side-chain lysyl benzyl-aminated peptides, the dissociation of the ion to form a benzylic carbocation $[C_7H_7]^+$ and a free primary ε-amine on the lysyl side chain (CCE pathway) is preserved when the precursor is protonated at the secondary ε-amino group of the derivatized residue (Scheme 1).[13]

In the present study on *o*-hydroxybenzyl-aminated peptides, the spectra displayed in Figs. 2 and 3 suggest that CCE is not the lone mechanism acting to break the C_ζ–N_ε bond. Some key features in the spectra which provide insight into the mechanisms involved include: (1) Aside from the presence of a low-intensity peak representing a y_6^{2+} ion observed in the MS/MS spectrum of the triply charged precursor ion of $IGK_{o\text{-}OH}GVAR$ (Fig. 3(B)), there is essentially no other evidence of amide backbone cleavage for the peptides analyzed in this study. (2) The overwhelming majority of the product ion current arises from fragmentation pathways involving cleavage of the C_ζ–N_ε bond. The CCE pathway results in elimination of the hydroxybenzyl moiety as a carbocation, $[C_7H_7O_1]^+$, while one or more alternative pathways eliminates the moiety as a neutral product, $[C_7H_6O]$. (3) Regardless of the mechanism involved in cleaving the C_ζ–N_ε bond, the resulting peptide product ions $[(MH_n)^{n+} - (C_7H_7O_1)^+]^{(n-1)+}$ and $[(MH_n)^{n+} - C_7H_6O_1]^{n+}$ exist as unmodified protonated peptide ions with the lysyl residue reclaiming its normal side-chain primary ε-amino structure.

Drawing upon these observations and prior knowledge of the fragmentation of benzylammonium ions (discussed above), the formation of the $[C_7H_7O_1]^+$ and $[(MH_n)^{n+} - (C_7H_7O_1)^+]^{(n-1)+}$ ions likely occur via the CCE pathway as illustrated by Path A in Scheme 2. Path A highlights the key features of the CCE pathway including the requirement for protonation at the secondary ε-amino group of the derivatized residue. This weakens the C_ζ–N_ε bond and direct heterolytic cleavage proceeds through an ion-neutral complex intermediate (INT1) producing a carbocation $[C_7H_7O_1]^+$ and an unmodified peptide product. For the formation of

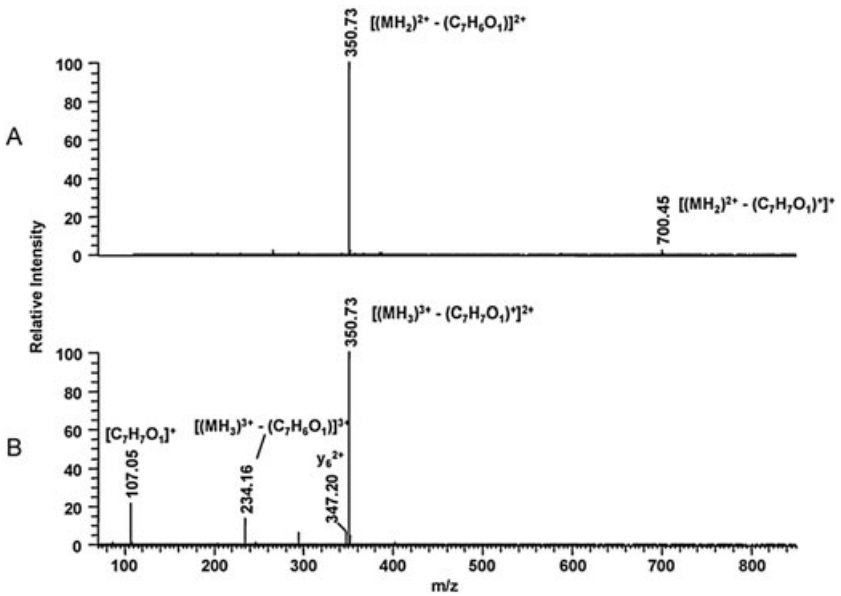

Figure 3. CID tandem mass spectra of the *ortho*-hydroxybenzyl-derivatized peptide $IGK_{o\text{-}OH}GVAR$ (where $K_{o\text{-}OH}$ represents the *ortho*-hydroxybenzyl-aminated lysyl residue). (A) CID MS/MS product ion spectrum of the doubly charged $[MH_2]^{2+}$ precursor ion. (B) CID MS/MS product ion spectrum of the triply charged $[MH_3]^{3+}$ precursor ion.

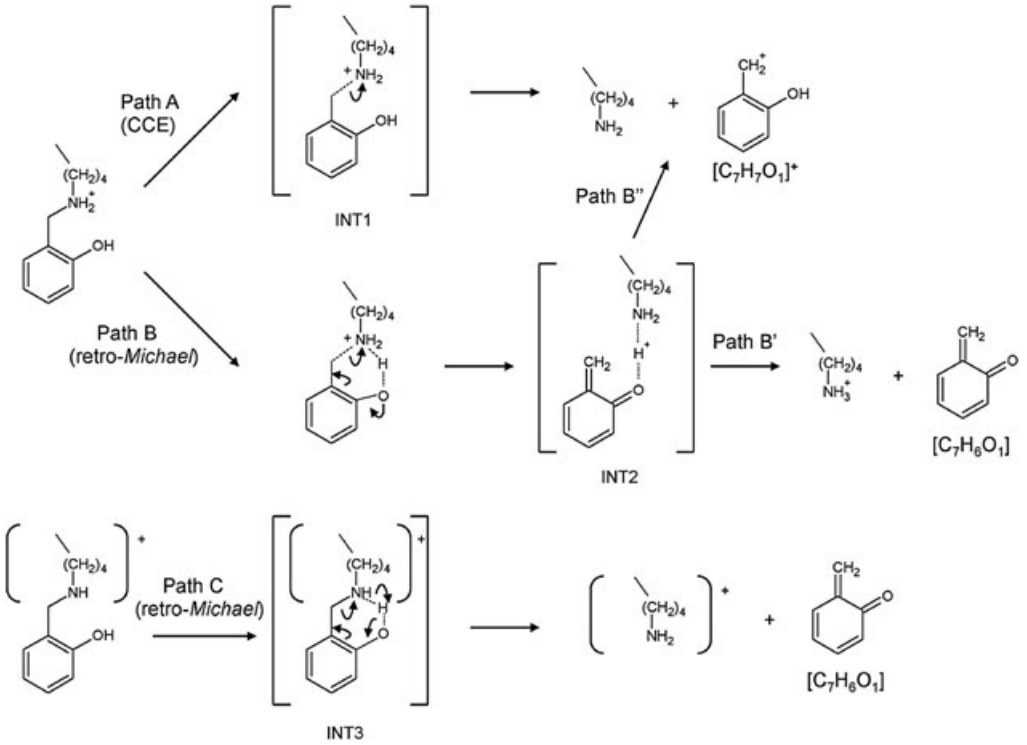

Scheme 2. Proposed dissociation pathways accounting for the selective side chain cleavage of *ortho*-hydroxybenzyl-aminated lysyl residues.

$[C_7H_6O_1]$, Paths B and C represent two variations of an alternative fragmentation pathway, an intramolecular retro-*Michael*-type reaction mechanism, for cases when the secondary ε-amino group is protonated (Path B) and not protonated (Path C), respectively. A retro-*Michael* mechanism was considered since it has been determined previously to be a viable dissociation pathway for 2-hydroxybenzyl-*N*-pyrimidinylamine derivatives where it was shown that the *o*-hydroxyl group initiates cleavage of the analogous C–N bond.[15] First considering Path B, protonation of N_ε induces a lengthening/weakening of the C_ζ–N_ε bond.[13] Concomitant with C_ζ–N_ε bond cleavage and electron rearrangement, hydrogen bonding of the proton from the *o*-OH group bridges the O atom at the *ortho*-position to N_ε of the developing primary amine (INT2). Separation of the protonated primary amine from the hydroxybenzyl moiety of INT2 produces the protonated primary ε-amine and a cyclic/conjugated ketone $[C_7H_6O_1]$ (Path B′). Alternatively, it was considered that INT2 could separate with the proton remaining with the hydroxybenzyl moiety forming CCE products (Path B″). For Path C, it was proposed that the hydrogen from the *o*-hydroxyl group is bridged to N_ε of the neutral secondary ε-amino group (INT3) through hydrogen bonding. This induces a weakening of the C_ζ–N_ε bond and subsequent substitution of $[C_7H_6O_1]$ by the proton at N_ε. Path C seems unlikely since the secondary ε-amino group is likely to have a relatively high gas-phase proton affinity and would be protonated. However, other factors can influence where ionizing protons reside (e.g. steric effects, electrostatic interactions, or hydrogen bonds) and such factors could inhibit protonation at the secondary ε-amino group. If hydrogen bonding does occur as represented by INT3, then protonation at the secondary ε-amino group may not be as likely.

Tandem mass spectra of *meta*-hydroxylated benzyl-derivatized peptides

To gain further insight into the possible role of the *o*-hydroxyl group in the intramolecular elimination of the hydroxybenzyl moiety $[C_7H_6O_1]$ at the ε-amino group (Paths B and C in Scheme 2), we analyzed the corresponding *m*-hydroxyl analogs. Figures 4(A) and 4(B) display tandem mass spectra of the doubly and triply charged precursor ions of the peptide $HAK_{m\text{-}OH}LGR$, respectively. Unlike the *o*-hydroxyl analog, the MS/MS spectrum for the doubly charged *m*-hydroxyl analog (Fig. 4(A)) displays a prevalence of amide backbone cleavage product ion peaks along with the peptide product ion peak $[(MH_2)^{2+} - (C_7H_7O_1)^+]^+$ originating from the CCE pathway. In the MS/MS spectrum of the triply charged precursor, the peaks representing the ions $[(MH_3)^{3+} - (C_7H_7O_1)^+]^{2+}$ and $[C_7H_7O_1]^+$ correspond to products formed exclusively from the CCE pathway (Fig. 4(B)). No evidence for the formation of $[C_7H_6O_1]$ was observed. This strongly supports the *o*-hydroxyl group playing a key role in the neutral loss of $[C_7H_6O_1]$ in CID of *o*-hydroxybenzyl-aminated peptide ions as described by Paths B and C of Scheme 2.

Optimized, low-energy structures of singly protonated N_ε-*ortho*-hydroxybenzyl glycyllysine ($GK_{o\text{-}OH}$)

To investigate the plausibility of the mechanisms displayed in Scheme 2, we adopted the simple peptide $GK_{o\text{-}OH}$ to perform DFT calculations for the determination of low-energy structures for singly protonated isomers and corresponding

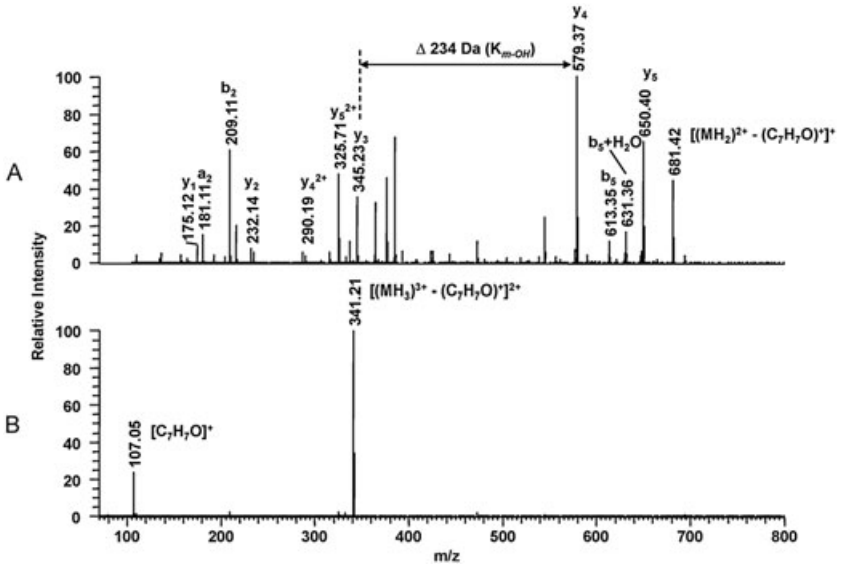

Figure 4. CID tandem mass spectra of the *meta*-hydroxybenzyl-derivatized peptide HAK$_{m\text{-}OH}$LGR (where K$_{m\text{-}OH}$ represents the *meta*-hydroxybenzyl-aminated lysyl residue). (A) CID MS/MS product ion spectrum of the doubly charged $[MH_2]^{2+}$ precursor ion. (B) CID MS/MS product ion spectrum of the triply charged $[MH_3]^{3+}$ precursor ion.

activation barriers associated with the proposed pathways. GK$_{o\text{-}OH}$ allowed for the comparison of the theoretical low-energy conformations for isomers protonated at the secondary ε-amino group of the derivatized lysyl residue, [GK$_{o\text{-}OH}$, ε]$^+$, and the N-terminal primary α-amino group, [GK$_{o\text{-}OH}$, α]$^+$ (displayed in Scheme 3). Additionally, we determined the low-energy conformations of GK$_{o\text{-}OH}$ protonated at the amide oxygen, [GK$_{o\text{-}OH}$, O]$^+$, and nitrogen, [GK$_{o\text{-}OH}$, N]$^+$, atoms between the glycyl and derivatized lysyl residues. Isomers [GK$_{o\text{-}OH}$, O]$^+$ and [GK$_{o\text{-}OH}$, N]$^+$ were considered to evaluate the likelihood of protonation along the amide backbone for peptides with the presumably high gas-phase proton affinity (see discussion above) associated with the secondary ε-amino group of the hydroxybenzyl modification. This could provide some insight into the lack of sequence ion peaks observed for *o*-hydroxybenzyl-aminated peptides (Figs. 2 and 3) since amide oxygen and nitrogen atoms of underivatized peptides can be protonated under conditions typically encountered in low-energy ion trapping and CID and protonated amide nitrogen atoms have been shown to weaken amide bonds resulting in subsequent cleavage via the b$_m$ – y$_n$ pathway.[22–24]

Table 1 lists the total energies (ZPVE corrected) resulting from DFT calculations for each of the four protonated isomers and the neutral counterpart of GK$_{o\text{-}OH}$. The total energy of neutral GK$_{o\text{-}OH}$ was used to calculate the site-specific gas-phase proton affinity for each of the isomers. Reflective of its significantly higher gas-phase proton affinity, protonation at the secondary ε-amino group, [GK$_{o\text{-}OH}$, ε]$^+$, produces the lowest energy structure. The second most stable structure corresponds to [GK$_{o\text{-}OH}$, α]$^+$ with protonation at the N-terminal amino group. [GK$_{o\text{-}OH}$, α]$^+$ has a total energy that is 19.1 kcal/mol higher than [GK$_{o\text{-}OH}$, ε]$^+$. For perspective, theoretical studies of the singly protonated dipeptide KG showed that the lowest energy conformer for protonation at the side-chain lysyl primary ε-amino group was only 3.5 kcal/mol lower in energy than the corresponding low-energy conformer for protonation at the N-terminal

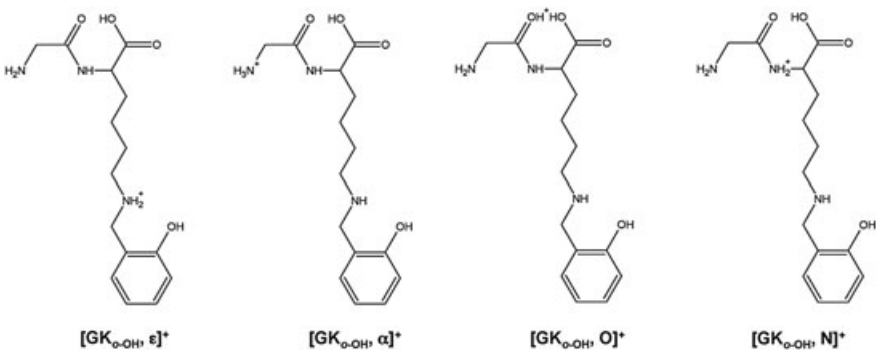

Scheme 3. Structures of singly-protonated isomers of the *ortho*-hydroxybenzyl-derivatized model peptide GK$_{o\text{-}OH}$.

Table 1. Total (ZPVE corrected) and relative energies of optimized, low-energy structures (determined at the B3LYP/6-31 + G (d,p) level of theory) of singly protonated species of $GK_{o\text{-}OH}$ displayed in Scheme 3. Corresponding site-specific gas-phase proton affinities (PA) and C_ζ–N_ε bond lengths are also listed for each structure

Species	Total energy (a.u.)	E_{rel} (kcal/mol)	PA (kcal/mol)*	C_ζ-N_ε bond length (Å)
$[GK_{o\text{-}OH}, \varepsilon]^+$	-1050.698129	0.0	231.1	1.52
$[GK_{o\text{-}OH}, \alpha]^+$	–1050.667722	19.1	212.0	1.48
$[GK_{o\text{-}OH}, O]^+$	–1050.666045	20.1	210.9	1.48
$[GK_{o\text{-}OH}, N]^+$	–1050.648794	31.0	200.1	1.48
$GK_{o\text{-}OH}$	–1050.329925	NA	NA	1.48

*Calculated using the total energy of the neutral structure of $GK_{o\text{-}OH}$.

primary amino group.[23] This implies that for *o*-hydroxybenzyl-aminated lysyl-containing peptides, protonation of the derivatized lysyl side chain is even more preferred than for underivatized lysyl residues. Moreover, the greater disparity in total energy between protonation at the secondary ε-amino group and the other sites suggests that a high activation barrier may inhibit intramolecular proton transfer reactions which ultimately initiate backbone cleavage via the b_m – y_n pathway.[22,25] This is supported by the MS/MS spectra of *o*-hydroxybenzyl-aminated lysyl-containing peptides which exhibit very little evidence for amide backbone cleavage reactions (Figs. 2 and 3). It should be pointed out that our goal in the investigation of the potential energy surface of $GK_{o\text{-}OH}$ was simply to establish a general picture for where ionizing protons are most likely to reside. The simple peptide model $GK_{o\text{-}OH}$ dismisses guanidinyl groups of arginyl residues (where one of the multiple protons would likely be sequestered) allowing us to compare the general order of other structural moieties where the remaining protons may prefer to reside. However, we are aware that, in addition to gas-phase proton affinity, other factors likely contribute (e.g. steric effects, electrostatic interactions, etc.) to the presence of other minima within the potential energy surface for each isomer, allowing some conformers of $[GK_{o\text{-}OH}, \varepsilon]^+$ to be closer in energy to some conformers of $[GK_{o\text{-}OH}, \alpha]^+$ and $[GK_{o\text{-}OH}, O]^+$.[23]

Based on the results in Table 1, the high gas-phase proton affinity of the secondary ε-amino group and the higher overall stability of $[GK_{o\text{-}OH}, \varepsilon]^+$ together suggest that most of the multiply protonated *o*-hydroxybenzyl-aminated peptide ions analyzed in this study would be protonated at the secondary ε-amino group of the derivatized residue. This appears to preclude Path C (Scheme 2) as a viable dissociation pathway. However, insight indicating the contrary can be extracted upon inspection of the optimized low-energy structures of $[GK_{o\text{-}OH}, \varepsilon]^+$ and $[GK_{o\text{-}OH}, \alpha]^+$ (Scheme 4). For $[GK_{o\text{-}OH}, \varepsilon]^+$, the C_ζ–N_ε bond is lengthened to 1.52 Å and the hydrogen atom of the *o*-OH group of the benzyl ring is oriented in an opposing direction relative to the protonated secondary amine N_ε atom. These observations suggest dissociation via the CCE pathway (Path A) may be favored. However, when $GK_{o\text{-}OH}$ is not protonated at the secondary ε-amino group ($[GK_{o\text{-}OH}, \alpha]^+$ in Scheme 4), the C_ζ–N_ε bond is shorter (1.48 Å) and the hydrogen atom of the *o*-OH group

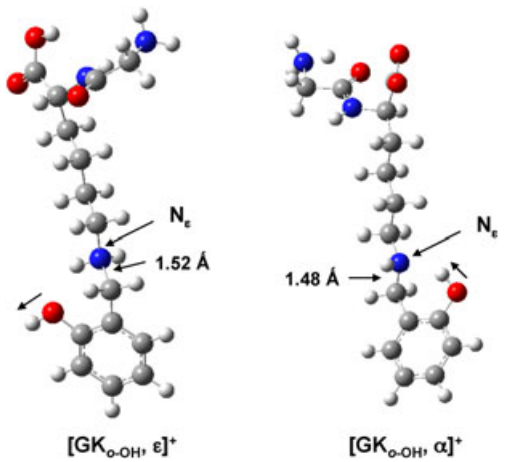

Scheme 4. Optimized low-energy structures for the singly-protonated isomers of $GK_{o\text{-}OH}$ protonated at the side chain secondary ε-amino group of the *ortho*-hydroxybenzyl-derivatized lysyl residue ($[GK_{o\text{-}OH}, \varepsilon]^+$) and N-terminal primary α-amino group ($[GK_{o\text{-}OH}, \alpha]^+$) respectively.

of the benzyl ring is oriented toward N_ε accompanied by a large amplitude O–H bond vibrational mode. The high gas-phase proton affinity of N_ε appears to promote a strong nucleophilic interaction with the hydrogen atom of the neighboring hydroxyl group. This orientation and a similar large amplitude vibrational mode was also observed for $[GK_{o\text{-}OH}, O]^+$ and $[GK_{o\text{-}OH}, N]^+$ (not shown) which were also not protonated at the secondary ε-amino group. The strong interaction between neutral N_ε and the hydrogen atom of the neighboring hydroxyl group in $[GK_{o\text{-}OH}, \alpha]^+$ introduces two notable considerations: (1) Path C in Scheme 2 may be feasible assuming some copies of protonated $GK_{o\text{-}OH}$ are not protonated. (2) The attraction of the proton of the *o*-OH group for the neutral N_ε atom could have a shielding effect that reduces the susceptibility of the secondary ε-amino group from acquiring an ionizing proton. The shielding effect reduces the effective proton affinity of the secondary ε-amino group relative to the theoretical value calculated (Table 1) and may allow for more abundant protonation at the N-terminal primary amino group or the amide oxygen atoms than suggested from the calculations.

Rapid Communications in Mass Spectrometry

Estimation of transition state activation barriers

DFT calculations were performed on the model peptide $GK_{o\text{-}OH}$ to estimate the transition state barriers associated with the proposed pathways in Scheme 2. Figure 5(A) displays the three-dimensional optimized structures at key points of the dissociation pathways described by Paths A and B of Scheme 2 for the model peptide protonated at the secondary ε-amino group, $[GK_{o\text{-}OH}, \varepsilon]^+$. Figure 5(B) displays a schematic illustrating key points (corresponding to the structures in Fig. 5(A)) along the potential energy surface of $[GK_{o\text{-}OH}, \varepsilon]^+$ for each dissociation pathway. Protonation lengthens the C_ζ–N_ε bond to 1.52 Å (compared to 1.48 Å when N_ε is not protonated) suggesting weakening and susceptibility to cleavage upon activation. For the theoretical investigation of the CCE pathway (Path A), the C_ζ–N_ε bond was stretched incrementally and constrained at each step while allowing all other degrees of freedom to relax. As displayed in Fig. 5(B) for Path A, cleavage of the C_ζ–N_ε bond via the CCE pathway passes through an activation barrier of 38.0 kcal/mol. No saddle points (intermediates) were evident along the potential energy surface during CCE suggesting no reverse barrier. The lack of a reverse activation barrier (or the presence of a practically indistinct minimum in the potential energy surface between reactants and products) is typical for related ions that dissociate through loose ion-neutral complexes including benzylpyridinium ions[26,27] and *N*-alkyl-*N*-benzylammonium ions.[21]

Path B in Scheme 2 describes an alternate pathway for precursor ions protonated at the secondary ε-amino group, which results in cleavage of the C_ζ–N_ε bond producing the neutral species $[C_7H_6O_1]$. We propose an intramolecular retro-*Michael*-type reaction in which a proton originating from the *o*-OH group replaces the hydroxybenzyl moiety at N_ε. This is supported by tandem mass spectra of the corresponding *m*-hydroxybenzyl analogs (Fig. 3), which exhibit no evidence for loss of $[C_7H_6O_1]$. Path B in Fig. 5(A) shows three-dimensional structures of $[GK_{o\text{-}OH}, \varepsilon]^+$ at key points of the retro-*Michael* pathway. As described for the

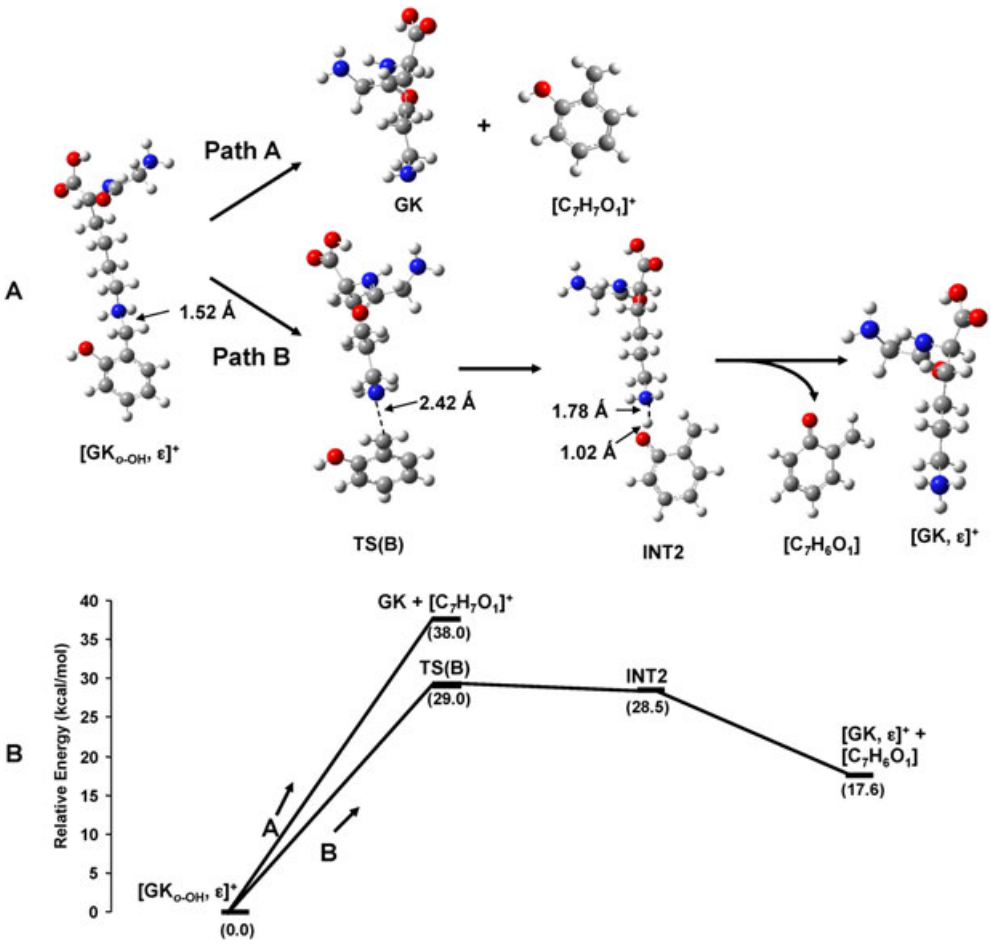

Figure 5. (A) Optimized three-dimensional structures corresponding to key points of the reactions of $[GK_{o\text{-}OH}, \varepsilon]^+$ dissociating via the CCE (Path A) and retro-*Michael* (Path B) pathways. (B) Schematic illustrating key points along the potential energy surface of $[GK_{o\text{-}OH}, \varepsilon]^+$ dissociating via the CCE (Path A) and retro-*Michael* (Path B) pathways. The points are associated with the corresponding three-dimensional structures illustrated in (A). Note: The transition state structure in Path B (TSB) is also a structure observed in Path A for the direct cleavage of the C_ζ–N_ε bond. At a bond length of 2.42 Å, the C_ζ–N_ε bond either continues to stretch (Path A) or a rotation of the hydroxybenzyl ring initiates Path B.

CCE pathway, during activation the C_ζ–N_ε bond stretches (already weakened due to protonation at N_ε). It is worthwhile to emphasize again that the hydrogen atom of the *o*-OH bond is oriented away from the N_ε atom. However, when the C_ζ–N_ε bond length reaches 2.42 Å, rearrangement of lone pair electrons of the *o*-hydroxyl group induces cleavage of the C_ζ–N_ε bond at a transition-state activation barrier of 29.0 kcal/mol, TS(B). This is accompanied by a rotation of the benzyl ring bringing the proton of the *o*-hydroxyl group within proximity to form a hydrogen bond bridge to the incipient primary ε-amine (INT2). The O–H bond of the *o*-hydroxyl group is extended significantly (1.02 Å) compared to the O–H bond length in phenol (0.96 Å)[28] demonstrating the attraction of the proton to N_ε. As shown in Scheme 2, the loose complex INT2 could dissociate to form the protonated primary amine and $[C_7H_6O_1]$ (Path B′) or the corresponding neutral amine and carbocation (Path B″). Analogous to the proton-bound dimers formed during amide backbone fragmentation where a shared proton bridges an oxazolone (b_m fragment) to a departing y_n fragment, the more favorable thermochemical products will be formed.[22] As implied by the reaction scheme in Fig. 5(B), the total relative energies of the retro-*Michael* products [GK, ε]$^+$ and $[C_7H_6O_1]$ are 17.6 kcal/mol while the CCE products GK and $[C_7H_7O_1]^+$ are 38.0 kcal/mol above the energy minimum of the precursor $[GK_{o\text{-}OH}, \varepsilon]^+$. The reaction scheme also shows that there is no activation barrier to form the retro-*Michael* products (Path B) once the intermediate INT2 is reached. This concurs with MS/MS spectral evidence of the doubly charged precursors (Figs. 2 and 3) where the retro-*Michael* pathway is clearly preferred. Triply charged precursors, on the other hand, exhibit products formed from both pathways even though our calculations demonstrate the retro-*Michael* pathway is more favorable. The simple, singly protonated $GK_{o\text{-}OH}$ model peptide adopted for the DFT calculations in this study is an effective approach to compare competing pathways. In reality, larger peptides have significantly more vibrational degrees of freedom, which facilitate numerous additional secondary interactions between various chemical moieties. Also, larger peptides can accommodate multiple protonation sites whereas $GK_{o\text{-}OH}$ is essentially restricted to a single protonation-induced charge due to Coulombic repulsion. These are just a few factors that cannot be addressed in the simple $GK_{o\text{-}OH}$ model but very well could be contributing influences on the relative occurrence of the two pathways. One possible explanation for the observed increase in the CCE pathway for triply charged precursors could be that it is driven by charge separation.

Figure 6(A) displays three-dimensional structures determined for the model peptide $[GK_{o\text{-}OH}, \alpha]^+$ at key points of dissociation via the retro-*Michael* pathway described by Path C in Scheme 2. Figure 6(B) displays a schematic illustrating key points (corresponding to the structures in Fig. 6(A)) along the potential energy surface of $[GK_{o\text{-}OH}, \alpha]^+$ during the reaction. The total energies in Fig. 6(B) are given relative to the low-energy conformer for the most stable

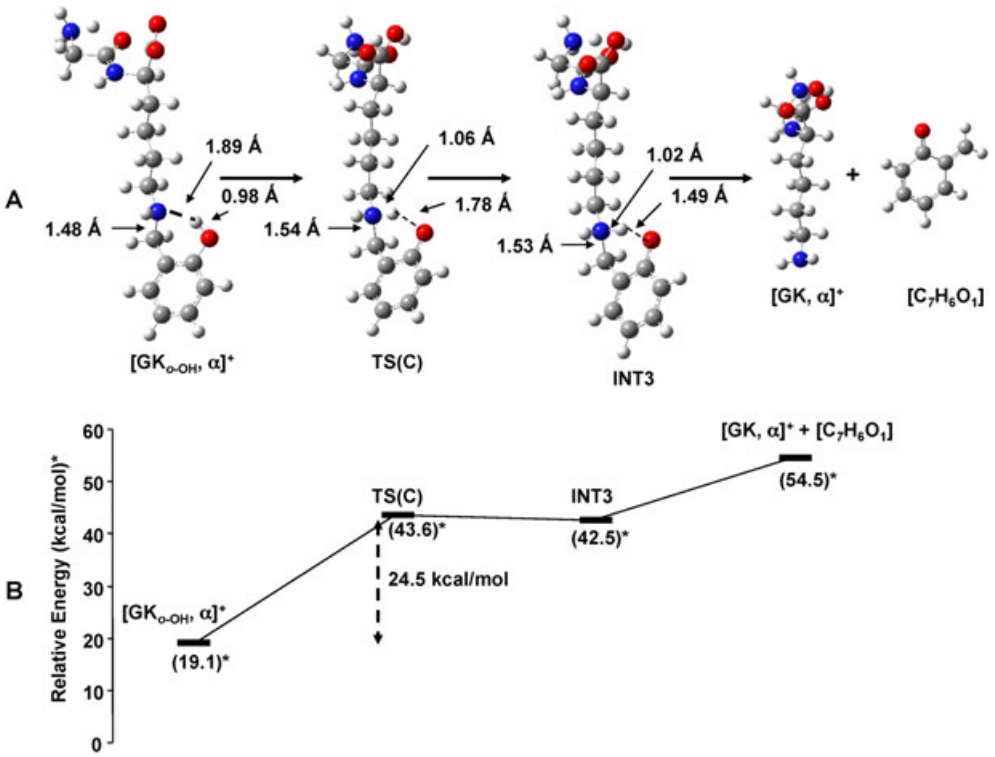

Figure 6. (A) Optimized three-dimensional structures corresponding to key points of the reaction of $[GK_{o\text{-}OH}, \alpha]^+$ dissociating via the retro-Michael pathway. (B) Schematic illustrating key points along the potential energy surface of $[GK_{o\text{-}OH}, \alpha]^+$ dissociating via the retro-Michael pathway. The points are associated with the corresponding three-dimensional structures illustrated in (A). * The total energies are given relative to the lowest energy structure of the most stable isomer $[GK_{o\text{-}OH}, \varepsilon]^+$.

Rapid Communications in Mass Spectrometry

Table 2. Transition state (TS) activation barriers determined in previous studies for simple peptides dissociating via amide cleavage reactions ($a_1 - y_1$ and b_1-ion formation) and those determined in this study for the *o*-hydroxybenzyl-aminated model peptide $GK_{o\text{-}OH}$ (displayed in Scheme 3) dissociating via the CCE and retro-*Michael* pathways

Precursor	Pathway	Product 1	Product 2	TS (kcal/mol)	Reference
KG	b_1-ion formation	α-amino-ε-caprolactam	Gly	39.4	[22]
VK	$a_1 - y_1$	a_1	y_1	43.7	[29]
$[GK_{o\text{-}OH}, \varepsilon]^+$	CCE	GK	$[C_7H_7O_1]^+$	38.0	*
$[GK_{o\text{-}OH}, \varepsilon]^+$	retro-*Michael*	$[GK, \varepsilon]^+$	$[C_7H_6O_1]$	29.0	*
$[GK_{o\text{-}OH}, \alpha]^+$	retro-*Michael*	$[GK, \alpha]^+$	$[C_7H_6O_1]$	24.5	*

*Determined theoretically in the present study.

isomer $[GK_{o\text{-}OH}, \varepsilon]^+$. With the secondary ε-amino group unprotonated, $[GK_{o\text{-}OH}, \alpha]^+$ has a shorter C_ζ–N_ε bond than $[GK_{o\text{-}OH}, \varepsilon]^+$ and the *o*-O–H bond is characterized by a large amplitude vibrational mode oriented in the direction of N_ε. Upon activation, the *o*-O–H bond length increases from 0.98 Å to 1.78 Å as the proton approaches closer to N_ε. Concomitantly, the C_ζ-N_ε bond length increases from 1.48 Å to 1.54 Å as the ion reaches the transition state, TS(C), with an activation barrier of 24.5 kcal/mol. The C_ζ–N_ε bond relaxes slightly to a length of 1.53 Å as the reaction passes through a shallow minimum in the potential energy surface represented by the intermediate structure INT3. INT3 then dissociates to the final products GK and $[C_7H_6O_1]$ with no reverse barrier.

DISCUSSION

The theoretically determined activation barriers for the selective side-chain cleavage of the C_ζ–N_ε bond of *o*-hydroxybenzyl-aminated lysyl-containing peptides by the pathways investigated in this study are listed in Table 2. Also listed are previously determined barriers for amide cleavage reactions of other simple, singly protonated peptides. The relative magnitude of the barriers in Table 2 provides strong support for our proposed fragmentation pathways (Scheme 2) being the active dissociation channels for *o*-hydroxybenzyl-aminated lysyl-containing peptides. The activation barriers for the CCE and retro-*Michael* pathways are lower than for those determined for amide cleavage reactions and this coincides with the experimental data, which exhibits little evidence for amide cleavage products (Figs. 2 and 3). As for the activation barriers associated with C_ζ–N_ε bond cleavage, the retro-*Michael* pathway is more kinetically favored compared to the CCE pathway and this also coincides with the experimental data in Figs. 2 and 3. For doubly charged precursors, products of the retro-*Michael* pathway were observed almost exclusively. CCE products become more prominent in the CID of triply charged precursor ions but charge separation likely plays a key role in making the CCE pathway more competitive with the retro-*Michael* pathway in that case.

CONCLUSIONS

This study describes the CID fragmentation characteristics of *o*-hydroxybenzyl-aminated lysyl-containing peptides. Two complementary mechanisms are involved in the selective cleavage of the C_ζ–N_ε bond connecting the derivative to the lysyl side chain. The CCE pathway results in the elimination of a hydroxybenzyl carbocation $[C_7H_7O_1]^+$ from the derivatized side chain while the retro-*Michael* pathway eliminates a conjugated cyclic ketone $[C_7H_6O_1]$. These limited fragmentation characteristics suggest that the *o*-hydroxybenzyl analog could represent a useful template for the development of reagents suited for specific applications where selective and predictable cleavage reactions are desired.

Acknowledgements

This research was supported by the NCRR (P41 RR018627) to P.C.A. We would also like to thank the Charles Brooks research group in the University of Michigan Chemistry Department for access to their computer cluster and Sun Corp. for donation of a Sunfire X4600 M2 computer.

REFERENCES

[1] D. F. Hunt, J. R. Yates, J. Shabanowitz, S. Winston, C. R. Hauer. Protein sequencing by tandem mass spectrometry. *Proc. Natl. Acad. Sci. USA* **1986**, *83*, 6233.
[2] D. N. Perkins, D. J. C. Pappin, D. M. Creasy, J. M. Cottrell. Probability-based protein identification by searching sequence databases using mass spectrometry data. *Electrophoresis* **1999**, *20*, 3551.
[3] J. K. Eng, A. L. McCormack, J. R. Yates III. An approach to correlate tandem mass spectral data of peptides with amino acid sequences in a protein database. *J. Am. Soc. Mass Spectrom.* **1994**, *5*, 976.
[4] D. Fenyö, R. C. Beavis. A method for assessing the statistical significance of mass spectrometry-based protein identifications using general scoring schemes. *Anal. Chem.* **2003**, *75*, 768.
[5] A. Sinz. Chemical cross-linking and mass spectrometry to map three-dimensional protein structures and protein-protein interactions. *Mass Spectrom. Rev.* **2006**, *25*, 663.
[6] B. Schilling, R. H. Row, B. W. Gibson. MS2Assign, automated assignment and nomenclature of tandem mass spectra of chemically crosslinked peptides. *J. Am. Soc. Mass Spectrom.* **2003**, *14*, 834.
[7] K. Kim, Y. Kim. Preparing multiple-reaction monitoring for quantitative clinical proteomics. *Expert Rev. Proteomics* **2009**, *6*, 225.
[8] G. E. Reid, K. D. Roberts, R. J. Simpson. Selective identification and quantitative analysis of methionine containing peptides by charge derivatization and tandem mass spectrometry. *J. Am. Soc. Mass Spectrom.* **2005**, *16*, 1131.

[9] Y. Lu, M. Tanasova, B. Borhan, G. E. Reid. Ionic reagent for controlling the gas-phase fragmentation reactions of cross-linked peptides. *Anal. Chem.* **2008**, *80*, 9279.
[10] F. Dreiocker, M. Q. Müller, A. Sinz, M. Schäfer. Collision-induced dissociative chemical cross-linking reagent for protein structure characterization: applied Edman chemistry in the gas phase. *J. Mass Spectrom.* **2010**, *45*, 178.
[11] P. A. C. Diego, B. Bajrami, H. Jiang, Y. Shi, J. A. Gascon, X. Yao. Site-preferential dissociation of peptides with active chemical modification for improving fragment ion detection. *Anal. Chem.* **2010**, *82*, 23.
[12] A. Lesur, E. Varesio. B. Domon, G. Hopfgartner. Peptides quantification by liquid chromatography with matrix-assisted laser desorption/ionization and selected reaction monitoring. *J. Proteome Res.* **2012**, *11*, 4972.
[13] E. S. Simon, P. G. Papoulias, P. C. Andrews. Gas-phase fragmentation characteristics of benzyl-aminated lysyl-containing tryptic peptides. *J. Am. Soc. Mass Spectrom.* **2010**, *21*, 1624.
[14] E. S. Simon, P. G. Papoulias, P. C. Andrews. Substituent effects on the gas-phase fragmentation reactions of protonated peptides containing benzylamine-derivatized lysyl residues. *Rapid Commun. Mass Spectrom.* **2012**, *26*, 631.
[15] H. Wang, X. Zang, Y. Guo. Mass spectrometric studies of the gas phase retro-*Michael* type fragmentation reactions of 2-hydroxybenzyl-*N*-pyrimidinylamine derivatives. *J. Am. Soc. Mass Spectrom.* **2005**, *16*, 1561.
[16] M. J. Frisch, G.W. Trucks, H.B. Schlegel, G.E. Scuseria, M.A. Robb, J.R. Cheeseman, J.A. Montgomery, T. Vreven, K.N. Kudin, J.C. Burant, J.M. Millam, S.S. Iyengar, J. Tomasi, V. Barone, B. Mennucci, M. Cossi, G. Scalmani, N. Rega, G.A. Petersson, H. Nakatsuji, M. Hada, M. Ehara, K. Toyota, R. Fukuda, J. Hasegawa, M. Ishida, T. Nakajima, Y. Honda, O. Kitao, H. Nakai, M. Klene, X. Li, J.E. Knox, H.P. Hratchian, J.B. Cross, V. Bakken, C. Adamo, J. Jaramillo, R. Gomperts, R.E. Stratmann, O. Yazyev, A.J. Austin, R. Cammi, C. Pomelli, J.W. Ochterski, P.Y. Ayala, K. Morokuma, G.A. Voth, P. Salvador, J.J. Dannenberg, V.G. Zakrzewski, S. Dapprich, A.D. Daniels, M.C. Strain, O. Farkas, D.K. Malick, A.D. Rabuck, K. Raghavachari, J.B. Foresman, J.V. Ortiz, Q. Cui, A.G. Baboul, S. Clifford, J. Cioslowski, B.B. Stefanov, G. Liu, A. Liashenko, P. Piskorz, I. Komaromi, R.L. Martin, D.J. Fox, T. Keith, M.A. Al-Laham, C.Y. Peng, A. Nanayakkara, M. Challacombe, P.M.W. Gill, B. Johnson, W. Chen, M.W. Wong, C. Gonzalez, J.A. Pople. *Gaussian 03, Revision C.02*, Gaussian, Inc., Wallingford, CT, **2004**.
[17] A. R. Katritzky, C. H. Watson, Z. Dega-Szafran, J. R. Eyler. Collisionally activated dissociation of *N*-alkylpyridinium cations to pyridinium cation and olefins in the gas phase. *J. Am. Chem. Soc.* **1990**, *112*, 2479.
[18] A. R. Katritzky, C. H. Watson, Z. Dega-Szafran, J. R. Eyler. Collisionally activated dissociation of *N*-alkylpyridinium cations to pyridine and alkyl cations in the gas phase. *J. Am. Chem. Soc.* **1990**, *112*, 2471.
[19] E. Anders, R. Koch, A. R. Katritzky, N. Malhotra, J. R. Eyler, J. A. Zimmerman. Collisionally activated dissociation of some bulkily substituted pyridinium cations, substituent effect on appearance potential. *Chem. Ber.* **1992**, *125*, 177.
[20] E. Zins, D. Rondeau, P. Karoyan, C. Fosse, S. Rochut, C. Pepr. Investigation of the fragmentation pathways of benzylpyridinium ions under ESI/MS conditions. *J. Mass Spectrom.* **2009**, *44*, 1668.
[21] V. D. Knyazev, S. E. Stein. Classical trajectories and RRKM modeling of collisional excitation and dissociation of benzylammonium and *tert*-butyl benzylammonium ions in a quadrupole-hexapole-quadrupole tandem mass spectrometer. *J. Am. Soc. Mass Spectrom.* **2010**, *21*, 425.
[22] B. Paizs, S. Suhai. Fragmentation pathways of protonated peptides. *Mass Spectrom. Rev.* **2005**, *24*, 508.
[23] I. P. Csonka, B. Paizs, G. Lendvay, S. Suhai. Proton mobility and main fragmentation pathways of protonated lysylglycine. *Rapid Commun. Mass Spectrom.* **2001**, *15*, 1457.
[24] B. Paizs, I. P. Csonka, G. Lendvay, S. Suhai. Proton mobility in protonated glycylglycine and N-formylglycylglycinamide: a combined quantum chemical and RKKM study. *Rapid Commun. Mass Spectrom.* **2001**, *15*, 637.
[25] V. H. Wysocki, G. Tsaprailis, L. L. Smith, L. A. Breci. Mobile and localized protons: a framework for understanding peptide dissociation. *J. Mass Spectrom.* **2000**, *35*, 1399.
[26] C. Collette, E. De Pauw. Calibration of the internal energy distribution of ions produced by electrospray. *Rapid Commun. Mass Spectrom.* **1998**, *12*, 165.
[27] V. Gabelica, E. De Pauw. Internal energy and fragmentation of ions produced in electrospray sources. *Mass Spectrom. Rev.* **2005**, *24*, 566.
[28] D. J. V. A. dos Santos, A. S. Newton, R. Bernardino, R. C. Guedes. Substituent effects on O-H and S-H bond dissociation enthalpies of disubstituted phenols and thiophenols. *Int. J. Quantum Chem.* **2008**, *108*, 754.
[29] C. Bleiholder, B. Paizs. Competing gas-phase fragmentation pathways of asparagine-, glutamine-, and lysine-containing dipeptides. *Theor. Chem. Acc.* **2010**, *125*, 387.

